Orientation Mechanism of $REBa_2Cu_3O_y$ (RE = Nd, Sm, Gd, Y, Yb) Thin Films Prepared by Pulsed Laser Deposition

Yusuke Ichino, Kimihiko Sudoh, Koji Miyachi, Yutaka Yoshida, and Yoshiaki Takai

***Abstract*—The orientation behavior and mechanism of $REBa_2Cu_3O_y$ (RE123) films have not been clarified yet. We prepared RE123 films by the pulsed laser deposition method and investigated the orientation behavior and mechanism. We argue that the orientation behavior strongly depends on thermodynamic parameters such as the heat of sublimation. The thickness and surface morphology dependences of the orientation suggest that c-axis oriented thicker films will be obtained in RE123 if the surface remains smooth up to objective thickness. Critical temperatures were around or higher than 90 K and critical current densities were larger than 1 MA/cm^2 for all RE123 films. From the viewpoint of the orientation, the Yb123 films were the easiest to grow with the c-axis normal to the substrate surface.**

***Index Terms*—Orientation mechanism, $REBa_2Cu_3O_y$, superconducting wire, thin film.**

I. Introduction

RECENTLY, the development of superconducting wire application employing $YBa_2Cu_3O_y$ (Y123) has been making great progress. In order to obtain μm order thick film, it is important to investigate the mechanisms of the epitaxial orientation. Many researchers have made an effort to explain the orientation behavior of the Y123 thin film. Mukaida *et al.* discussed the substrate dependence of the orientation of the Y123 film [1]. They showed and summarized that mixed a- and c-axis orientations were caused by a well lattice matched substrate and a low substrate temperature. The orientation depended on the geometric configuration of the substrate lattice and the Y123 lattice. However, the novel orientation behaviors of Nd123 thin films have three kind of the region of the orientation in the temperature-oxygen pressure phase diagram [2], [3], and Yb123 thin films are dominantly c-axis orientation in the almost all deposition conditions (this work). Those unfamiliar orientations can not be explained with the existing data. In the present work, we deposited the RE123 thin films (RE = Sm, Gd, Y, Yb) by the pulsed laser deposition technique and considered the orientation behavior of the RE123 thin films systematically, and then surface morphologies and superconducting properties also were investigated.

Manuscript received August 5, 2002.

Y. Ichino, Y. Yoshida and Y. Takai are with the Department of Electronics, Nagoya University, Furo-cho, Chikusa-ku, Nagoya 464-8603, Japan (e-mail: y-ichino@mbox.media.nagoya-u.ac.jp).

K. Sudoh and K. Miyachi are with the Department of Energy Engineering and Science, Nagoya University, Furo-cho, Chikusa-ku, Nagoya 464-8603, Japan.

Digital Object Identifier 10.1109/TASC.2003.811972

II. Experimental Procedure

A. Target Preparation

We have used the $REBa_2Cu_3O_y$ (RE123, RE = Sm, Gd, Y, and Yb) sintered bulk material as target. The RE123 targets were synthesized by a conventional solid reaction method in air. The starting materials were high purity (99.99%) RE_2O_3, BaO_2 and CuO. Appropriate amounts were accurately weighted and thoroughly mixed. The mixed powder was pressed into pellets and sintered first at 800, 900 and 990°C for 12 h with two intermediate grindings and pressing in air, respectively. We identified the phase in the targets using an x-ray diffraction. The samples except for RE = Yb became the pure RE123 phase. Although the phases of RE = Yb sample were mainly Yb_2BaCuO_x (Yb211), Ba–Cu–O compounds and a very small amount of Yb123 phases, the thin films deposited with that target were successfully grown of only the Yb123 phase.

B. Film Preparation and Characterization

The RE123 thin films were prepared by the usual pulsed laser deposition technique on (100) MgO substrate with the sintered targets. Deposition conditions are listed in Table I. Substrates were heated by the radiation of the ceramic heater and the substrate temperatures were checked with the radiation pyrometer.

The crystallinity and orientation of the RE123 films were checked by θ–2θ x-ray diffraction with a Cu-Kα source. Here, orientations of the films were defined by a diffraction intensity ratio of (200) to $(200) + (005)$. The surface of the films was imaged by an atomic force microscopy (AFM). The composition and thickness of the films were confirmed with the inductively coupled plasma spectroscopy. We measured superconducting properties of the films with the conventional dc four-probe method in high magnetic fields $(B//c,\ B = 0–9\ \mathrm{T})$. Before these measurements, silver pads were deposited as electrodes on the films, which were then annealed at 350–400°C for 1–3 hours in O_2 gas flow to ensure good contacts. The T_c values were determined by adopting a voltage criterion of 2 μV/cm with the current density of 100 A/cm^2. The voltage criterion for J_c was same with that for T_c measurement.

III. Results and Discussion

A. Orientation Behavior and Mechanism

We firstly investigated the substrate temperature (T_s) and the oxygen pressure $pO_2)$ dependences of the orientation of the

TABLE I
THE DEPOSITIONAL CONDITION OF THE RE123 THIN FILMS

Parameters	*Conditions*
Target	RE123 sintered bulk
Substrate	(100)MgO, (100)$SrTiO_3$
Substrate Temperature	650 - 850°C
Oxygen Pressure ($p\,O_2$)	6.7 - 133.3 Pa
Substrate-Target distance	50 mm
Laser Source	ArF (λ = 193 nm)
Laser Energy	1.0 J/cm^2
Laser Repetition Rate	10 Hz

RE123 films as summarized in Fig. 1. The behavior of orientation change was different among the RE123 films. The Y123 orientation varied from dominantly c-axis orientated one to a, c-mixed one with decreasing T_s. In the case of Nd123 films, although the orientations were similar to those of Y123 at high T_s, the c-axis orientation appeared at further low T_s, again. In other words, the orientations of the Nd123 films were classified into three regions by high, middle and low T_s regions. On the other RE123 films (RE $=$ Sm, Gd and Yb), the orientation boundaries between dominantly c-axis orientation and a, c-mixed one were represented by chain dashed circles as drawn in Fig. 1.

We investigated the film thickness dependence of the film orientation as seen in Fig. 2 so that those complex behaviors of the orientations also were affected by the film thickness. As shown in Fig. 2, the a-axis intensity ratio of the films deposited at low T_s increases monotonically with increasing the film thickness. While the films deposited at high T_s keeps up the c-axis orientation. We suppose a simple model as drawn in Fig. 2 inset. This model argues that the a, c-mixed orientation consists of the c-axis oriented layer just above the substrate and the a-axis oriented layer on the c-axis one. The stacking sequence and the initial growth stage of the Y123 and Nd123 films on several substrates (MgO, $SrTiO_3$ and $LaAlO_3$) were investigated by many workers [4]–[7]. According to them, the c-axis oriented ultra thin layer existed on the interface since the initial layers of the RE123 films tend to become the CuO, Cu_2O or BaO layer. These studies support our growth model.

Using our model, we considered the nucleation of the a-axis and c-axis domains. Here, we assumed the 2D nucleation occurred on the c-axis oriented layer in the initial growth stage. When a 2D nucleus with radius r forms, the total Gibbs energy change $\Delta G(r)$ on the nucleation can be written as following equation,

$$\Delta G(r) = -\frac{\pi h r^2}{v}\Delta\mu + 2\pi h r \sigma_{\rm lat} + \pi r^2\left(\sigma_{\rm bas} + \sigma_{\rm inter} - \sigma_{(001)}\right). \quad (1)$$

Here, h, v and σ represents a height of the nucleus, a volume of the unit cell of RE123 and a surface free energy per unit area. $\Delta\mu$ is a chemical potential change per a molecule between a vapor and a solid phase. The $\sigma_{(001)}$ and $\sigma_{\rm inter}$ represent a surface energy of the underlying c-axis layer and an interfacial energy between the nucleus and the underlying RE123. The terms

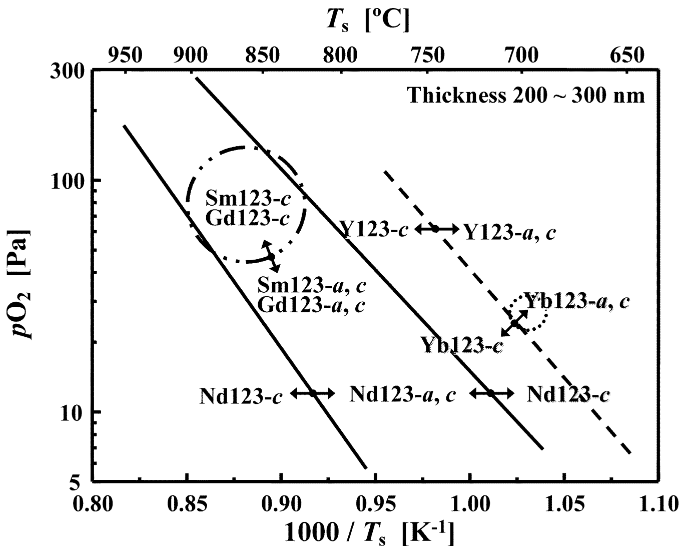

Fig. 1. Schematic drawing of the orientational behaviors of the RE123 films as functions of T_s and pO_2. Lines and circles represent the boundary of the orientation, and i in RE123-i show the preferential orientational direction of the RE123 films. The Nd123 films' data was referred from [2], [3], which were deposited on $SrTiO_3$ substrates. The thickness of these films was 200–300 nm.

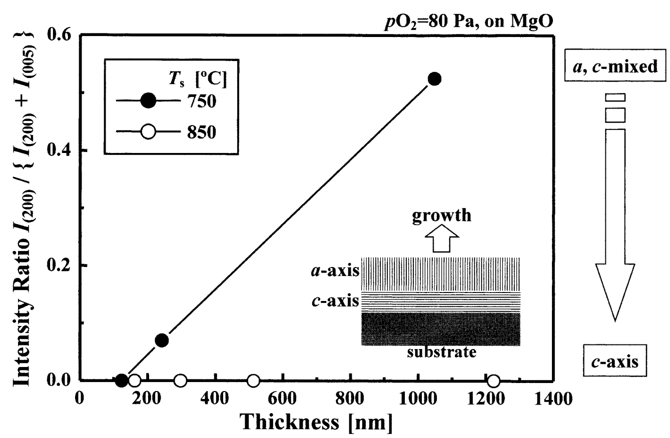

Fig. 2. Orientations of the Yb123 thin films as a function of the thickness. The vertical axis represents the peak intensity ratio of $I_{(200)}$ to $I_{(200)} + I_{(005)}$. The inset shows the cross sectional picture of the a, c-mixed orientation.

$\sigma_{\rm bas}$ and $\sigma_{\rm lat}$ are a basal and a lateral surface energy of the nucleus. Granozio *et al.* discussed the surface free energies of fully deoxidized Y123 crystal using the *ab-initio* calculations and the indentation method [8], [9]. According to this literature, the surface free energies were 0.82 J/m^2 for the (100) plane and 0.59 J/m^2 for (001) plane. In the case of nucleation on Y123 (001) surface, $\sigma_{\rm inter}$ for each orientation case are also calculated, $\sigma_{\rm inter} \approx 0.23$ J/m^2 for a-axis oriented nucleus while $\sigma_{\rm inter} = 0$ for c-axis one. Those values for RE123 have not been confirmed yet. Thus, we employed σ's of Y123 in present work. The critical Gibbs free energy ΔG^* of a nucleus are obtained from $\partial(\Delta G)/\partial r = 0$. Therefore, ΔG^* are represented by

$$\Delta G^* = \frac{\pi (h\sigma_{\rm lat})^2}{\left(\frac{h}{v}\right)\Delta\mu - \left(\sigma_{\rm bas} + \sigma_{\rm inter} - \sigma_{(001)}\right)}. \quad (2)$$

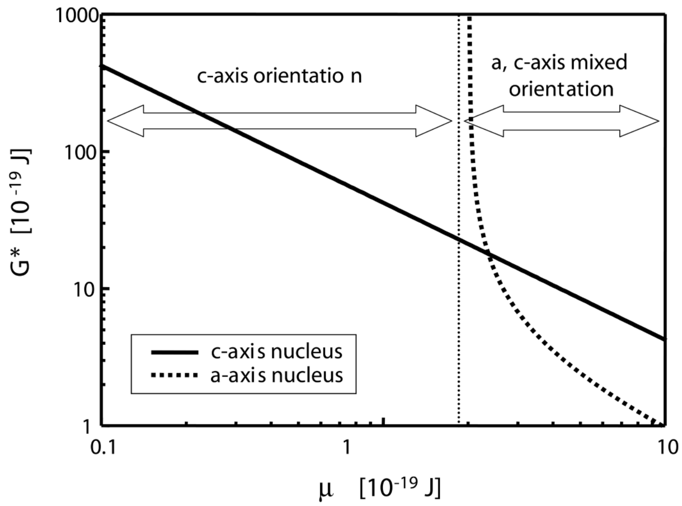

Fig. 3. Critical nucleation energy on the c-axis oriented layer as a function of the chemical potential change. The a, c-mixed orientation occurs, when $\Delta\mu$ is larger than certain threshold value.

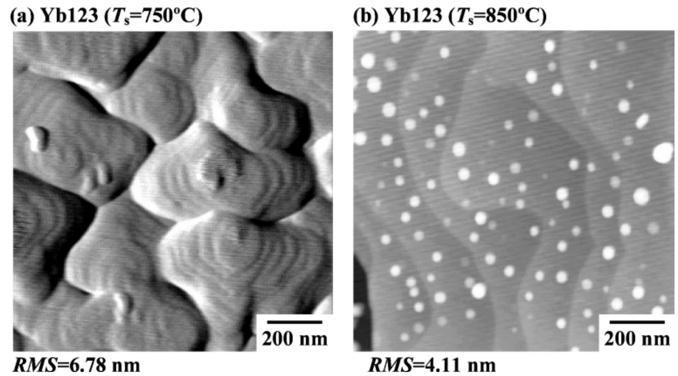

Fig. 4. Surface morphologies of Yb123 films deposited on (100)MgO at (a) $T_s = 750°C$ and (b) $T_s = 850°C$. These thicknesses were about 200 nm. The former growth mode was the 2D island, while the latter one was the step flow.

ΔG^* corresponds to a thermodynamic barrier with respect to the nuclei growing up. If this value is low, the nucleation easily occurs. We plotted the ΔG^*'s as a function of $\Delta\mu$ in Fig. 3. This figure shows that both of the a- and c-axis oriented nuclei are generated on grounds that the films are deposited at high $\Delta\mu$ conditions, which correspond to low T_s and pO_2. Consequently, the orientations of those films become the a, c-mixed. This behavior of ΔG^* is universal and independent of the RE123 kind to the extent that the surface energy of (001) plane is smaller that that of (100) plane.

$\Delta\mu$ depends on a heat of sublimation Δh and an entropy change Δs between a vapor and a solid phase as follows,

$$\Delta\mu = \Delta h - T\Delta s. \quad (3)$$

Here Δh and Δs are the values per molecule and T is the temperature of the nucleation system. Since Δh's are related to the peritectic temperature, a low peritectic temperature of certain RE123 results in a low Δh, and then the orientation of these films will facilitate to become the c-axis. In facts, the Yb123 films, which have low peritectic temperature about 900°C, showed the c-axis orientation over a wide range of growth conditions. Vice versa, the c-axis oriented Nd123 films required higher T_s further than those of other RE123 films because of high peritectic temperature. However, the complete comprehension of the orientation behaviors needs to consider not only the thermodynamic causation such as our model as mentioned above, but also kinetics of the adatoms.

B. Surface Morphology

The surface morphology also depends on RE123 materials and the growth condition. We show surface AFM images of Yb123 films in Fig. 4. It can be seen that the film deposited at $T_s = 750°C$ had 2D island growth, while the other one showed the morphology of the step flow. The step heights of both films were one unit cell (~1.2 nm). With increasing T_s, the surface of Yb123 films became flat. Here, it may be considered that a high T_s results in the low $\Delta\mu$ from (3). It is well known that $\Delta\mu$ affects the surface morphologies such as the step width of the spiral growth [10]. The deposition condition giving low $\Delta\mu$ contributes to producing a flat surface. From this view point, the Yb123 material has the possibility of the most flat surface among the RE123 because of the low peritectic temperature.

Notice that the $T_s = 850°C$ film maintained the c-axis orientation up to at least 1.2 μm in Fig. 2. This suggests that maintaining a smooth surface is necessary for the c-axis orientated thicker film. In other words, the a, c-mixed orientation is also introduced by the rough surface. Hence, to obtain the c-axis oriented thicker film with high critical current (I_c), we must choose the suitable RE123 material which maintains a smooth surface up to desired thickness.

C. Superconducting Properties

We characterized the superconducting properties of the RE123 films with usual dc four-probe method. The Sm123 and Gd123 films, which feature solid solutions represented by $RE_{1+x}Ba_{2-x}Cu_3O_y$, were made up from $x \geq 0$ targets. The properties of these films are described elsewhere in more detail [11]–[13]. The critical temperature (T_c) of our all films was about 90 K higher. In the case of thin films, the T_c's among RE123 did not differ noticeably compared to bulk. In practice, those values of Sm123 and Gd123 revealed 90–93 K, while Yb123 was about 90 K.

Next, we measured J_c's in magnetic fields (B) applied parallel to the crystallographic c-axis of the films from 0 up to 9 T. As shown in Fig. 5, J_c decreased with increasing B for all RE123 systems. Interestingly, in low magnetic fields less than 1 T, the J_c of Sm123 film which consisted of slightly Sm rich composition was superior to other RE123 films [12]. We consider that the refined solid solutions dispersing in Sm123 film contribute to this excellent property. Within range of the magnetic fields from 1 to 5 T, the J_c-B dependence was similar for all RE123 films. On the other, we measured the J_c of Yb123 film decayed steeper than other RE123 films in high magnetic fields over 6 T. Typical J_c value of RE123 film is much greater than that of bulk since many crystal defects contained in the film act as strong pinning center. Additionally, RE-Ba substitution region is present in Sm123 and Gd123 film. Hence the pinning force of the Yb123 films is weaker than that of Sm123 and Gd123 film. However, we consider that there are no objections about the application of Yb123 films up to middle magnetic fields.

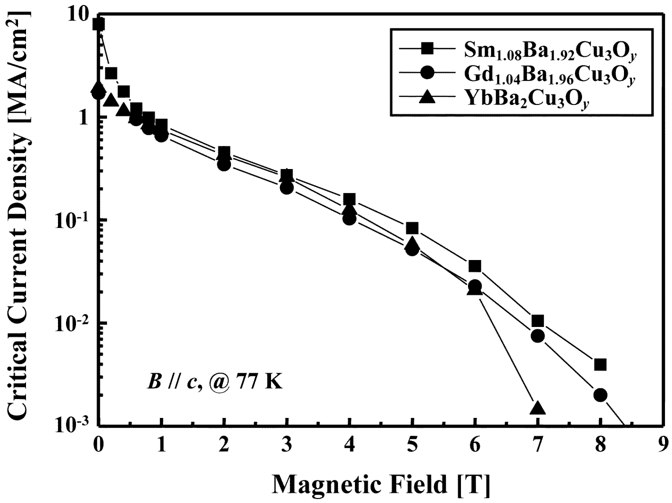

Fig. 5. Critical current densities of RE123 films (RE = Sm, Gd and Yb) as a function of magnetic fields applied perpendicular to the substrate surfaces.

IV. Conclusion

We systematically investigated the orientations and the superconducting properties of RE123 thin films. We found that Yb123 films can easily grow in the c-axis orientation with relatively good superconducting properties. The properties of Yb123 films can be advantageous in producing the superconducting wire. We must select the suitable RE123 material in accordance with the requirement.

Acknowledgment

This work was performed using facilities of the Materials Design and Characterization Laboratory, Institute for Solid State Physics, University of Tokyo.

References

[1] M. Mukaida and S. Miyazawa, "Preferential axis control of $YBa_2Cu_3O_x$ thin film by quasilattice-match engineering," *J. Appl. Phys.*, vol. 74, no. 2, pp. 1209–1212, 1993.

[2] Y. Ichino *et al.*, "Preparation of $NdBa_2Cu_3O_x$ thin films and their superconducting properties in magnetic fields," *Advances in Supercond.*, vol. 12, pp. 879–881, 2000.

[3] H. Zama, K. Ishikawa, T. Suzuki, and T. Morishita, "New growth conditions for the c-axis oriented $NdBa_2Cu_3O_x$ films by pulsed laser deposition: Lower substrate temperature and higher oxygen pressure," *Jpn. J. Appl. Phys.*, vol. 32, pp. L923–L925, 1999.

[4] R. Ramesh *et al.*, "The atomic structure of growth interfaces in Y–Ba–Cu–O thin films," *J. Mater. Res.*, vol. 6, pp. 2264–2271, 1991.

[5] M. Mukaida and S. Miyazawa, "Nature of preferred orientation of $YBa_2Cu_3O_x$ thin films," *Jpn. J. Appl. Phys.*, vol. 32, pp. 4521–4528, 1993.

[6] Y. Wu, Z. Hao, Y. Enomoto, and K. Tanabe, "Atomic configurations of $YBa_2Cu_3O_{7-x}$/MgO interfaces," *Physica C*, vol. 371, pp. 309–314, 2002.

[7] K. Hattori, S. Santo, Y. Yoshida, N. Matsunami, and Y. Takai, "Surface study of the initial growth of $NdBa_2Cu_3O_{7-y}$ thin films on MgO," *Advances in Supercond.*, vol. 12, pp. 972–974, 2000.

[8] F. M. Granozio and U. S. di Uccio, "Simple model for the nucleation of (001) and (100) oriented grains in YBCO films," *J. Crystal Growth*, vol. 174, pp. 409–416, 1997.

[9] F. M. Granozio, M. Shalluzo, U. S. di Uccio, I. Maggio-Aprile, and ø Fischer, "Competition between a-axis and c-axis growth in superconducting $RBa_2Cu_3O_{7-x}$ thin films," *Phys. Rev. B*, vol. 61, pp. 756–765, 2000.

[10] T. Nishinaga and H. J. Scheel, "Crystal growth aspect of high-T_c superconductors," *Advances in Supercond.*, vol. 8, pp. 33–38, 1996.

[11] K. Sudoh, Y. Yoshida, and Y. Takai, "Effect of deposition conditions and solid solution on the $Sm_{1+x}Ba_{2-x}Cu_3O_{6+\delta}$ thin films prepared by pulsed laser deposition," Physica C, to be published.

[12] K. Sudoh, Y. Ichino, M. Itoh, Y. Yoshida, Y. Takai, and I. Hirabayashi, "Correlation between film thickness and critical current density of $Sm_{1+}Ba_{2-x}Cu_3O_{6+\delta}$ films deposited by pulsed laser deposition," Jpn. J. Appl. Phys., to be published.

[13] K. Miyachi, Y. Ichino, K. Sudoh, Y. Yoshida, and Y. Takai, "The effect of substitution of Gd for Ba site in $Gd_{1+x}Ba_{2-x}Cu_3O_{6+\delta}$ thin films," Physica C, submitted for publication.